Atmos. Chem. Phys. Discuss., 13, 12263–12286, 2013
www.atmos-chem-phys-discuss.net/13/12263/2013/
doi:10.5194/acpd-13-12263-2013

Atmospheric Chemistry and Physics Discussions
Open Access

Stratospheric O_3 changes during 2001–2010: the small role of solar flux variations in a CTM

S. S. Dhomse[1], M. P. Chipperfield[1], W. Feng[1], W. T. Ball[2], Y. C. Unruh[2], J. D. Haigh[2], N. A. Krivova[3], S. K. Solanki[3], and A. K. Smith[4]

[1]School of Earth and Environment, University of Leeds, LS2 9JT Leeds, UK
[2]Imperial College, SW7 2AZ London, UK
[3]Max-Plank-Institut für Sonnensystemforschung, 37191 Katlenburg-Lindau, Germany
[4]National Center for Atmospheric Research, Boulder, CO 80307, USA

Received: 26 March 2013 – Accepted: 17 April 2013 – Published: 8 May 2013

Correspondence to: S. S. Dhomse (s.s.dhomse@leeds.ac.uk)

Published by Copernicus Publications on behalf of the European Geosciences Union.

Abstract

Solar spectral fluxes (or irradiance) measured by the SOlar Radiation and Climate Experiment (SORCE) show different variability at ultraviolet (UV) wavelengths compared to other irradiance measurements and models (e.g. NRL-SSI, SATIRE-S). Some modelling studies have suggested that stratospheric/lower mesospheric O_3 changes during solar cycle 23 (1996–2008) can only be reproduced if SORCE solar fluxes are used. We have used a 3-D chemical transport model (CTM), forced by meteorology from the European Centre for Medium-Range Weather Forecasts (ECMWF), to simulate middle atmospheric O_3 using three different solar flux datasets (SORCE, NRL-SSI and SATIRE-S). Simulated O_3 changes are compared with Microwave Limb Sounder (MLS) and Sounding of the Atmosphere using Broadband Emission Radiometry (SABER) satellite data. Modelled O_3 anomalies from all solar flux datasets show good agreement with the observations, despite the different flux variations. The off-line CTM reproduces these changes through dynamical information contained in the analyses. A notable feature during this period is a robust positive solar signal in the tropical middle stratosphere due to changes in stratospheric dynamics. Ozone changes in the lower mesosphere cannot be used to discriminate between solar flux datasets due to large uncertainties and the short time span of the observations. Overall this study suggests that, in a CTM, the UV variations detected by SORCE are not necessary to reproduce observed stratospheric O_3 changes during 2001–2010.

1 Introduction

The Sun is a primary source of energy to the Earth's atmosphere, so it is essential to understand the influence that solar flux variations may have on the climate system. This can be studied by investigating the effect of 11 yr solar flux variations on the atmosphere. Although total solar irradiance (TSI) shows only a small variation (~ 0.1 % per solar cycle), significant (up to 100 %) variations are observed in the ultra-violet

ACPD
13, 12263–12286, 2013

(UV) region of the solar spectrum. Therefore, in a "top-down" mechanism, these UV changes are thought to modify middle atmospheric (lower mesospheric and stratospheric) O_3 production, thereby indirectly altering background temperatures (for a review see Gray et al., 2010). These temperature changes can then modulate upward propagating planetary waves, and amplify the solar signal in stratospheric O_3 and temperatures. The temperature changes will also affect the rates of chemical reactions which control ozone.

This mechanism has been well accepted. For example, using Solar Back-scatter Ultraviolet Radiometer (SBUV, 1979–2003) and Stratospheric Aerosol and Gas Experiment II (SAGE II, 1984–2003) satellite data, Soukharev and Hood (2006) showed nearly +3 % O_3 variation in the upper stratosphere/lower mesosphere (45–55 km) with no solar signal in the tropical middle stratosphere (30–40 km). Randel and Wu (2007) estimated a similar signal using SAGE I and SAGE II (1979–2005) data. However, using Halogen Occultation Experiment (HALOE, 1992–2005) data, both Soukharev and Hood (2006) and Remsberg (2008) showed a negligible (< 1 %) O_3 solar signal in the upper stratosphere/lower mesosphere and a positive solar signal in the middle stratosphere.

These differences in the lower mesospheric and upper stratospheric ozone solar signal between SBUV, SAGE and HALOE have been attributed to the shorter time span (< 14 yr) of HALOE measurements (Soukharev and Hood, 2006). However, using an off-line 3-D chemical transport model (CTM) forced with European Centre for Medium-Range Weather Forecasts (ECMWF) (re)analysis meteorological data and NRL-SSI solar fluxes (Lean et al., 1997), Dhomse et al. (2011) found that their modelled solar signal was in better agreement with HALOE than SBUV or SAGE. Also, although some coupled 2-D and 3-D CCMs are able to simulate a "double-peak"-structured solar signal in tropical O_3, the simulated upper stratospheric peak is at lower altitudes than SBUV and SAGE observations (e.g. see Figure 4 in Austin et al., 2008) in almost all cases.

Recently, these differences in the middle atmospheric solar signal have gathered renewed interest with the availability of solar spectral data from the Solar Radiation and

ACPD
13, 12263–12286, 2013

Climate Experiment (SORCE), launched in 2003. These SORCE fluxes show significantly different variations compared to the NRL-SSI model. Using SORCE solar fluxes in a 2-D radiative-dynamical-chemical model, and comparing results with Microwave Limb Sounder (MLS) data, Haigh et al. (2010) argued that the upper stratospheric and lower mesospheric O_3 solar signal might be out of phase with TSI during solar cycle 23. Using the Whole Atmosphere Community Climate Model (WACCM) with these SORCE solar fluxes and comparing it with Sounding the Atmosphere using Broadband Emission Radiometry (SABER) data, Merkel et al. (2011) also showed an out-of-phase (larger than −2 %) day-time O_3 solar signal in the mesosphere and upper stratosphere (above 40 km) during the recent solar maximum. Importantly, both Haigh et al. (2010) and Merkel et al. (2011) argued that the recent O_3 changes in the upper stratosphere and lower mesosphere cannot be simulated using the NRL-SSI solar fluxes, thereby providing indirect evidence for the fidelity of the SORCE solar fluxes. However, although the WACCM-simulated mesospheric O_3 changes with SORCE fluxes showed better agreement with SABER data, the same model run was unable to simulate stratospheric O_3 changes (see Figure 2d and h in Merkel et al., 2011).

In this study we use the SLIMCAT off-line 3-D CTM forced with ECMWF ERA-interim meteorology to simulate recent stratospheric and lower mesospheric O_3 changes. Using different solar flux datasets and dynamical conditions, we examine whether the model can reproduce these past O_3 changes, and therefore whether the model comparisons can help establish the accuracy of the solar fluxes used. Section 2 gives a brief description of the various satellite O_3 and solar flux data sets used. Section 3 describes the model set up. Our results are discussed in Sect. 4, and conclusions are summarised in Sect. 5.

2 Satellite data sets and solar fluxes

The SABER instrument was launched in December 2001 on board the TIMED (Thermosphere Ionosphere Mesosphere Energetics and Dynamics) satellite. SABER is an

ACPD
13, 12263–12286, 2013

infrared radiometer and O_3 profiles are retrieved from the 1.27 µm band during the day and from the 9.6 µm band for both day and night. SABER therefore provides about 2200 profiles per 24 h period. Here we use O_3 profile data from the 9.6 µm band (v1.07) with anomalous O_3 profiles removed following Rong et al. (2009). Day-time and night-time measurements are separated using a flag provided in the data files. The vertical resolution of the SABER data is about 2 km with a useful vertical range between 10–0.0002 hPa (∼ 30–100 km)

MLS was launched onboard the Aura satellite in July 2004. MLS consists of seven radiometers covering spectral regions from 118 GHz to 2.5 THz. MLS provides about 3500 profiles per 24 h period covering both day and night. The vertical resolution of MLS data ranges from 3 km in the lower stratosphere to about 5.5 km in the lower mesosphere, with a useful vertical range between 100–0.02 hPa (∼ 16–70 km). MLS has retrieval errors of about 5 % in the middle and upper stratosphere and 10 % in the lower stratosphere (Froidevaux et al., 2008).

SATIRE-S is a semi-empirical model that calculates total and spectral solar irradiance variations (Krivova et al., 2003; Ball et al., 2012). It uses magnetograms and continuum images to identify three components that modulate solar irradiance: faculae, sunspot umbrae and sunspot penumbrae. The rest of the visible solar surface is considered to be the quiet Sun, which is thus the 4th component of the model. Semi-empirical models of the solar atmospheric structure are used to calculate the emergent intensities for each component (Unruh et al., 1999). Weighted by the corresponding area coverage these intensities are summed up to calculate spectral irradiance at a daily cadence. An Upper Atmosphere Research Satellite/Solar Ultraviolet Spectral Irradiance Monitor (UARS/SUSIM)-based correction is applied to wavelengths below 270 nm to gain better agreement with observations (Krivova et al., 2006).

The NRL-SSI solar flux model uses the photospheric sunspot index and the Mg II index to calculate the contribution of sunspots and faculae to irradiance changes, respectively (Lean et al., 1997). To calculate irradiance below 400nm, a regression with UARS/SOLSTICE (Solar Stellar Irradiance Comparison Experiment) observations

ACPD
13, 12263–12286, 2013

is performed. This is done on detrended, rotational data to avoid the introduction of long-term instrumental errors.

Both NRL-SSI and SATIRE-S solar flux data show very similar 11 yr solar cycle variability for wavelengths less than 250 nm. Above 250 nm, SATIRE-S displays larger variability, with twice the change in flux compared to NRL-SSI at 300 nm, increasing to a three-fold larger variation at 370 nm. For most wavelengths between 440 and 1250 nm NRL-SSI is more variable than SATIRE-S.

3 Model experiments

SLIMCAT is a 3-D CTM which uses a hybrid σ-θ vertical coordinate system. Model runs were performed at $5.6^{\circ} \times 5.6^{\circ}$ horizontal resolution with 32-vertical levels ranging from the surface to about 64 km (~ 0.1 hPa). The model was forced with 6-hourly (00:00, 06:00, 12:00 and 18:00 UTC) ERA-interim reanalysis data for 2001–2010. Vertical velocities are calculated using heating rates and the modelled O_3 (Chipperfield, 2006), so a heating-rate related dynamical response (Oberländer et al., 2012) is incorporated in the simulations. The model has a detailed stratospheric chemistry scheme and there are 203 spectral intervals in the UV-visible photolysis scheme from 116 to 850 nm (see WMO, 1985, Table 7-4).

We have performed seven model simulations with different solar flux datasets and dynamical conditions and these are summarised in Table 1. Run *A_NRL* used NRL-SSI fluxes (similar to run B_Int in Dhomse et al., 2011) while run *B_SATIRE* used SATIRE-S fluxes. Run *C_FIX* was similar but used the mean NRL-SSI fluxes for 2001–2010. This means that run *C_FIX* only includes meteorological variability (i.e. no solar flux variability). Due to significant gaps in the SORCE data timeseries, a multi-annual simulation could not be performed with these fluxes. Run *D_SORCE2004* and *E_SORCE2007* are therefore two separate 10 yr simulations with constant SORCE solar fluxes for December 2004 and December 2007, respectively. These are the same fluxes as used in the 2-D model study by Haigh et al. (2010). Runs *G_NRLF* and *F_SATIREF* are similar to

ACPD
13, 12263–12286, 2013

A_NRL and *B_SATIRE*, respectively but with fixed dynamics (from year 2004), these runs therefore contain solar variability but no meteorological variability.

4 Results and discussion

The differences in irradiance from the different solar flux datasets used in our model simulations are shown in Fig. 1. The threshold wavelength (242 nm) controlling O_3 production and destruction is also indicated. As shown in Haigh et al. (2010), at 210 nm SORCE data shows nearly 9 % more UV in December 2004 (solar maximum period) than in December 2007 (solar minimum period). However, NRL-SSI and SATIRE-S both show only about a 2 % difference between these two months at this wavelength. Recently, Woods (2012) and Ermolli et al. (2013) re-evaluated SORCE data and suggested that the UV variability detected by SORCE might be 50 % lower than shown in Fig. 1. DeLand and Cebula (2012) argued that the SORCE flux variations we show in Fig. 1 might be incorrect due to undercorrection of instrument response changes during early on-orbit measurements. This indicates ongoing uncertainty in the accuracy of the SORCE data. Nevertheless, we employ the available SORCE data, as used in Haigh et al. (2010), to test the impact on modelled ozone and examine whether this can provide indirect evidence for their accuracy.

There are significant differences between stratospheric and mesospheric O_3 chemistry. Stratospheric O_3 is dynamically controlled whereas there is a strong diurnal cycle in mesospheric O_3 via HO_x chemistry (e.g. Marsh et al., 2003). Figure 2 shows monthly mean tropical (25° S–25° N) day and night-time O_3 profiles from SABER and run *A_NRL*. Overall, there is good agreement between modelled and observed O_3 during both December 2004 and December 2007. However, the peak in modelled O_3 seems to be at a lower altitude and upper stratospheric O_3 values are slightly smaller than those from SABER. Daytime O_3 values are in good agreement in the lower mesosphere, but above 55 km modelled night-time O_3 mixing ratios are less than observed by SABER. The estimated amplitude of the O_3 diurnal cycle (day-time mean minus

ACPD
13, 12263–12286, 2013

night-time mean) is also shown in Fig. 2. As expected there are negligible differences in the stratosphere (up to 0.2 ppm, or less than 1 %). However, the amplitude of the diurnal cycle in modelled O_3 in the mesosphere above 55km seems to be slightly lower than those observed in SABER data.

Figure 3 shows tropical (25° S–25° N) O_3 anomalies at 0.3, 3 and 30 hPa from model runs *A_NRL*, *B_SATIRE*, and *C_FIX* (2001–2010) along with SABER (2002–2010) and MLS (2004–2010) observations. Excellent agreement among satellite and modelled O_3 anomalies is observed at the 3 levels with typical differences between them are less than 1 %. This is not surprising as middle-lower stratospheric O_3 is dynamically controlled and our simulations use realistic dynamics (including the QBO). Overall, the modelled O_3 anomalies are better correlated with MLS than SABER. For example, at 30 hPa and 3 hPa, the MLS-model correlation is 0.9 while for MLS-SABER it is 0.8, highlighting the differences in the observational data sets. The MLS-SABER differences are largest in 2005 and 2008. In general, prior to 2005, SABER O_3 anomalies are slightly smaller (< 0.5 %) than MLS and SLIMCAT at all levels and they become slightly larger afterwards.

The good correlation between modelled and satellite O_3 anomalies provides confidence in the middle and upper stratospheric O_3 changes during this period. However, the weaker correlations in the observational data sets in the lower mesosphere (0.3 hPa) (e.g. Mieruch et al., 2012), suggest that O_3 changes in this region must be carefully interpreted. Some model-SABER differences during the first few months of the SABER period might be due to reported ice build-up in the SABER detector during this time (Rong et al., 2009).

Zonal mean O_3 mixing ratios for December 2004 from SLIMCAT (runs *A_NRL* and *D_SORCE2004*), SABER and MLS are shown in Fig. 4. Results from run *B_SATIRE* are not shown as they are similar to run *A_NRL*. Although there is generally excellent agreement in the O_3 distribution, some differences in modelled and satellite O_3 in the tropical stratosphere are visible. In the middle stratosphere (near 10 hPa) MLS values are slightly smaller than SABER and SLIMCAT. In the lower stratosphere (below 50 hPa) and the lower mesosphere (above 1 hPa) SABER mixing ratios are larger than SLIMCAT and MLS.

Figure 4 also shows the relative O_3 differences between December 2004 and December 2007. Haigh et al. (2010) showed differences for day-time O_3 only (their Figure 2), whilst our differences shown in Fig. 4 include both day and night-time O_3. Also, Haigh et al. (2010) used a coupled dynamical-chemical 2-D model, so a direct comparison with their results cannot be performed. However, some differences in O_3 between the 2-D model and SLIMCAT (runs *A_NRL* as well as *D_SORCE2004* minus *E_SORCE2007*) are noticeable. As in Haigh et al. (2010) (with SORCE fluxes), a 2–4 % O_3 increase in the tropical middle stratosphere is clearly visible in all SLIMCAT simulations, confirming that the middle stratospheric enhancement can be simulated with NRL-SSI (or SATIRE), fixed and SORCE solar fluxes as the model uses realistic dynamics. However, significant O_3 reductions in the tropical upper stratosphere (above 1 hPa) produced in the 2-D model with SORCE solar fluxes are not visible in MLS, SABER or any SLIMCAT simulation. Note that run *D_SORCE2004* has larger O_3 mixing ratios than run *A_NRL* in December 2004. This is due to absolute differences between NRL-SSI and SORCE fluxes; the exact cause of this difference in solar fluxes is beyond the scope of this study.

Another interesting feature in Fig. 4 is the 10 % increase in O_3 between 0–30° N and 15–5 hPa, which is distinctly noticeable in the observations and is well captured by the model. The model also captures the ~10 % less O_3 between 5° S–5° N near 30 hPa, 20–40° S near 70 hPa, and 70–90° S near 20 hPa. However, there are differences in the SABER and MLS observations. Enhanced O_3 in the tropical lower stratosphere near 50 hPa is seen by MLS and the model, but does not appear in the SABER data. SABER also observed nearly 2 % less O_3 in the southern hemisphere (SH) mid-latitude upper stratosphere (above 0.3 hPa) which is not seen by MLS or reproduced by the model.

To analyse the effect of the diurnal cycle and for better comparison with Haigh et al. (2010), annual mean day and night-time O_3 differences between 2004 and 2007 with SORCE fluxes (runs *D_SORCE2004* minus *E_SORCE2007*) are shown in Fig. 5. A middle stratospheric O_3 enhancement of nearly +6 % during 2004 (near 5 hPa) is clearly visible in both day and night-time O_3 (see also Fig. 3h). Hence most of these O_3 changes must be due to dynamical changes. Interestingly these positive O_3 differences in the tropics are much larger than the 2-D model. However, at mid-high latitudes SLIMCAT shows negative differences (i.e. more O_3 in 2007) while the 2-D model showed nearly uniform positive differences throughout the stratosphere. These negative O_3 differences are distinctly visible between 40–60° N.

In the upper stratosphere and lower mesosphere SLIMCAT does not show any significant O_3 differences. However, in a fixed dynamics simulation (with SORCE fluxes) they are slightly negative during the day but become positive at night. For the mean solar signal in O_3 in the lower mesosphere these effects seem to cancel out. This is in disagreement with Merkel et al. (2011), who argued for an insignificant solar signal in night-time O_3, and thus an average O_3 solar signal remains negative.

Figure 6 shows day and night-time O_3 differences between 2003–2004 and 2008–2009 from model runs *A_NRL*, *B_SATIRE*, *C_FIX* and SABER. We have selected the pairs of years as active and quiet solar periods in order to make a direct comparison with the results from Merkel et al. (2011). Again, the O_3 difference patterns between observational and modelled data are nearly similar. The SABER data and all three model simulations show 3–6 % more O_3 in the tropical middle stratosphere during 2003–2004 compared to 2008–2009. Negative differences in the lower stratosphere (near 50 hPa) are also in agreement with the data and model runs. The simulations show negligible (< 1 %) O_3 differences in the upper stratosphere and lower mesosphere. SABER also shows nearly 0.5 % negative O_3 anomalies in a narrow region near 0.3 hPa in both day and night-time data. SH mid-latitude SABER-observed O_3 changes are better captured in run *B_SATIRE* than run *A_NRL*, whereas NH mid-latitude changes are in better agreement with run *A_NRL*. However, due to the limited spatial coverage of SABER measurements, mid-latitude O_3 differences are not discussed here.

As expected our analysis of SABER data shown in Fig. 6 is consistent with the active (2003/4) and quiet (2008/9) period O_3 differences shown in Figure 2 of Merkel et al.

ACPD
13, 12263–12286, 2013

(2011). However, the SLIMCAT O_3 differences do not agree with WACCM differences using NRL-SSI in that study. The tropical mid-stratospheric O_3 anomalies with NRL-SSI or SORCE solar fluxes shown by Merkel et al. (2011) are less than 1 %, whereas our simulations and SABER show O_3 differences of nearly 4 %. This again highlights that robust positive O_3 anomalies observed in SABER data can be reproduced in SLIMCAT with either NRL-SSI or SATIRE solar fluxes. Negligible upper stratospheric lower mesospheric O_3 changes with NRL-SSI are in good agreement with their simulations (see Figure 2a and e in Merkel et al., 2011).

Figure 7a shows the solar signals from some earlier studies (e.g. HALOE (Remsberg, 2008), a 2-D model (Brasseur, 1993) and a 3-D model (Dhomse et al., 2011)). A mid-stratospheric solar signal in earlier SLIMCAT simulations with NRL-SSI fluxes is consistent with other modelling studies (e.g. Austin et al., 2008, see Figure 4). Figure 7b shows the estimated solar signal in tropical (25° S–25° N) O_3 using modelled and observed O_3 anomalies from this study. The regression model used here is similar to the one used in Dhomse et al. (2011) containing linear trend, QBO and solar ($F_{10.7}$ flux) terms (see also Dhomse et al., 2006). Overall the solar signal from runs *A_NRL* and *B_SATIRE* are in good agreement with SABER (and HALOE) data. However, due to the short time span of available MLS data (77 months), the estimated errors in the MLS solar signal are much larger. A robust positive solar signal in the middle stratosphere is clearly visible in the model simulations as well as SABER and MLS data sets.

There are some differences in the solar signals estimated from modelled and observed O_3 in Fig. 7b, but they are statistically insignificant. For example, the secondary solar signal maxima in the tropical lower stratospheric O_3 observed in SBUV, SAGE and SLIMCAT is not visible in SABER and MLS data. In the upper stratosphere and lower mesosphere modelled O_3 shows a positive (~ 1 %) solar signal whereas in the observational data it is negative (~ –1 %). Some of these difference might be due to ice contamination in the SABER detector as discussed earlier.

Discussion Paper | Discussion Paper | Discussion Paper | Discussion Paper |

ACPD
13, 12263–12286, 2013

In Fig. 7c, the regression is applied for the 2003–2010 time period. Both runs *A_NRL* and *B_SATIRE* show a negative solar signal in the lower mesosphere. This clearly highlights the importance of the time period used to quantify the O_3 solar signal. Figure 7c also shows the "chemical-only" solar response for the 2001–2010 period from fixed dynamical simulations (runs *G_NRLF* and *F_SATIREF*). Again, the solar signal from these simulations shows quite good agreement with the solar signal from SAGE and SBUV data (Soukharev and Hood, 2006). However, its magnitude is less than that for the fixed dynamical simulations presented in Dhomse et al. (2011). This is in line with our expectations, as the 2001–2010 time period only partially covers the solar cycle.

5 Conclusions

When using either NRL-SSI or SATIRE-S solar fluxes, and ECMWF meteorology, simulated O_3 from our 3-D CTM shows excellent agreement with satellite observations for 2001–2010. The model is also able to reproduce changes over the recent 2004–2007 time period which has previously been used to support the different solar flux variability measured by SORCE. Therefore, our model runs do not provide any indirect support for the accuracy of the new SORCE fluxes; rather they argue that the previously accepted NRL-SSI or SATIRE-S fluxes are able to reproduce recent observed O_3 changes.

The good agreement between our model and observations is partly due to variability imposed by the ECMWF analyses, which is therefore dynamical in origin. However, since 2001, there have been step-wise changes in stratospheric circulation (e.g. Dhomse et al., 2008) and a major sudden stratospheric warming in the SH in September 2002 (e.g. Weber et al., 2003). It will require further research using a coupled chemistry-climate model to see if these anomalous changes in stratospheric circulation are indeed solar-induced or due to internal atmospheric variability.

Our modelled O_3 solar signal in the middle and upper stratosphere during the 2001–2010 time period is different to that deduced from SBUV or SAGE data (1979–2003),

ACPD
13, 12263–12286, 2013

but only slightly different (similar structure but larger in magnitude) than HALOE (1992–2005). However, there are some uncertainties in the SBUV (e.g. poor vertical resolution) and SAGE (e.g. limited temporal sampling, Twomey-Chahine inversion near 50 km) data sets (e.g. Terao and Logan, 2007; Wang et al., 2011). A re-evaluation of SBUV and SAGE data is needed to confirm if the solar signal in stratospheric O_3 during the recent solar cycle is indeed out of phase with TSI changes.

Acknowledgements. We thank NASA for the MLS and SABER O_3 data sets. We also acknowledge use of the ECMWF data which was obtained via the BADC. This work was supported by the NERC SOLCLI project, NCAS and NCEO. The National Center for Atmospheric Research is sponsored by the National Science Foundation.

References

Austin, J., Tourpali, K., Rozanov, E., Akiyoshi, H., Bekki, S., Bodeker, G., Bruehl, C., Butchart, N., Chipperfield, M., Deushi, M., Fomichev, V. I., Giorgetta, M. A., Gray, L., Kodera, K., Lott, F., Manzini, E., Marsh, D., Matthes, K., Nagashima, T., Shibata, K., Stolarski, R. S., Struthers, G. H., and Tian, W.: Coupled chemistry climate model simulations of the solar cycle in ozone and temperature, J. Geophys. Res., 113, D11306, doi:10.1029/2007JD009391, 2008. 12265, 12273

Ball, W. T., Unruh, Y., Krivova, N. A., Solanki, S., Wenzler, T., Mortlock, D. J., and Jaffe, A. H.: Reconstruction of total solar irradiance 1974–2009, Astron. Astrophys., 541, A27, doi:10.1051/0004-6361/201118702, 2012. 12267

Brasseur, G.: The response of the middle atmosphere to long-term and short-term solar variability: A two-dimensional model, J. Geophys. Res., 98, 23079–23090, 1993. 12273, 12286

Chipperfield, M. P.: New Version of the TOMCAT/SLIMCAT Off-Line Chemical Transport Model: Intercomparison of Stratospheric Tracer Experiments, Q. J. Roy. Meteor. Soc., 132, 1179–1203, 2006. 12268

DeLand, M. T. and Cebula, R. P.: Solar UV variations during the decline of Cycle 23, J. Atmos. Sol.-Terr. Phy., 77, 225–234, 2012. 12269

Dhomse, S., Weber, M., Wohltmann, I., Rex, M., and Burrows, J. P.: On the possible causes of recent increases in northern hemispheric total ozone from a statistical analysis of satellite data from 1979 to 2003, Atmos. Chem. Phys., 6, 1165–1180, doi:10.5194/acp-6-1165-2006, 2006. 12273

Dhomse, S., Weber, M., and Burrows, J.: The relationship between tropospheric wave forcing and tropical lower stratospheric water vapor, Atmos. Chem. Phys., 8, 471–480, doi:10.5194/acp-8-471-2008, 2008. 12274

Dhomse, S., Chipperfield, M. P., Feng, W., and Haigh, J. D.: Solar response in tropical stratospheric ozone: a 3-D chemical transport model study using ERA reanalyses, Atmos. Chem. Phys., 11, 12773–12786, doi:10.5194/acp-11-12773-2011, 2011. 12265, 12268, 12273, 12274, 12286

Ermolli, I., Matthes, K., Dudok de Wit, T., Krivova, N. A., Tourpali, K., Weber, M., Unruh, Y. C., Gray, L., Langematz, U., Pilewskie, P., Rozanov, E., Schmutz, W., Shapiro, A., Solanki, S. K., and Woods, T. N.: Recent variability of the solar spectral irradiance and its impact on climate modelling, Atmos. Chem. Phys., 13, 3945–3977, doi:10.5194/acp-13-3945-2013, 2013. 12269

Froidevaux, L., Jiang, Y. B., Lambert, A., Livesey, N. J., Read, W. G., Waters, J. W., Browell, E. V., Hair, J. W., Avery, M. A., Mcgee, T. J., Twigg, L. W., Sumnicht, G. K., Jucks, K. W., Margitan, J. J., Sen, B., Stachnik, R. A., Toon, G. C., Bernath, P. F., Boone, C. D., Walker, K. A., Filipiak, M. J., Harwood, R. S., Fuller, R. A., Manney, G. L., Schwartz, M. J., Daffer, W. H., Drouin, B. J., Cofield, R. E., Cuddy, D. T., Jarnot, R. F., Knosp, B. W., Perun, V. S., Snyder, W. V., Stek, P. C., Thurstans, R. P., and Wagner, P. A.: Validation of Aura Microwave Limb Sounder stratospheric ozone measurements, J. Geophys. Res., 113, D15S20, doi:10.1029/2007JD008771, 2008. 12267

Gray, L., Beer, J., M., G., Haigh, J., Lockwood, M., Matthes, K., Cubasch, U., Fleitmann, D., Harrison, G., Hood, L., Luterbacher, J., Meehl, G., Shindell, D., van Geel, B., and White, W.: Solar Influences on Climate, Rev. Geophys., 48, RG4001, doi:10.1029/2009RG000282, 2010. 12265

Haigh, J. D., Winning, A. R., Toumi, R., and Harder, J. W.: An influence of solar spectral variations on radiative forcing of climate, Nature, 467, 696–699, 2010. 12266, 12268, 12269, 12271

Krivova, N., Solanki, S., Fligge, M., and Unruh, Y. C.: Reconstruction of solar irradiance variations in cycle 23: Is solar surface magnetism the cause?, Astron. Astrophys., 399, 1–4, 2003. 12267

ACPD
13, 12263–12286, 2013

Solar cycle and stratospheric ozone

S. S. Dhomse et al.

Krivova, N., Solanki, S., and Floyd, L.: Reconstruction of solar UV irradiance in cycle 23, Astron. Astrophys., 452, 631–639, doi:10.1051/0004-6361:20064809, 2006. 12267

Lean, J. L., Rottman, G. J., Kyle, H. L., Woods, T. N., Hickey, J. R., and Puga, L. C.: Detection and parameterization of variations in solar mid- and near-ultraviolet radiation (200–400 nm), J. Geophys. Res., 102, 29939–29956, 1997. 12265, 12267

Marsh, D., Smith, A., and Noble, E.: Mesospheric ozone response to changes in water vapor, J. Geophys. Res., 108, 4109, doi:10.1029/2002JD002705, 2003. 12269

McLinden, C. A., Tegtmeier, S., and Fioletov, V.: Technical Note: A SAGE-corrected SBUV zonal-mean ozone data set, Atmos. Chem. Phys., 9, 7963–7972, doi:10.5194/acp-9-7963-2009, 2009. 12286

Merkel, A. W., Harder, J. W., Marsh, D. R., Smith, A. K., Fontenla, J. M., and Woods, T.: The impact of solar spectral irradiance variability on middle atmospheric ozone, Geophys. Res. Lett., 38, L13802, doi:10.1029/2011GL047561, 2011. 12266, 12272, 12273

Mieruch, S., Weber, M., von Savigny, C., Rozanov, A., Bovensmann, H., Burrows, J. P., Bernath, P. F., Boone, C. D., Froidevaux, L., Gordley, L. L., Mlynczak, M. G., Russell III, J. M., Thomason, L. W., Walker, K. A., and Zawodny, J. M.: Global and long-term comparison of SCIAMACHY limb ozone profiles with correlative satellite data (2002–2008), Atmos. Meas. Tech., 5, 771–788, doi:10.5194/amt-5-771-2012, 2012. 12270

Oberländer, S., Langematz, U., Matthes, K., Kunze, M., Kubin, A., Harder, J., Krivova, N. A., Solanki, S. K., Pagaran, J., and Weber, M.: The influence of spectral solar irradiance data on stratospheric heating rates during the 11 year solar cycle, Geophys. Res. Lett., 39, L01801, doi:10.1029/2011GL049539, 2012. 12268

Randel, W. J. and Wu, F.: A stratospheric ozone profile data set for 1979–2005: Variability, trends, and comparisons with column ozone data, J. Geophys. Res., 112, D06313, doi:10.1029/2006JD007339, 2007. 12265, 12286

Remsberg, E. E.: On the response of Halogen Occultation Experiment (HALOE) stratospheric ozone and temperature to the 11-year solar cycle forcing, J. Geophys. Res., 113, D22304, doi:10.1029/2008JD010189, 2008. 12265, 12273, 12286

Rong, P. P., Russell III, J. M., Mlynczak, M. G., Remsberg, E. E., Marshall, B. T., Gordley, L. L., and López-Puertas, M.: Validation of Thermosphere Ionosphere Mesosphere Energetics and Dynamics/Sounding of the Atmosphere using Broadband Emission Radiometry (TIMED/SABER) v1.07 ozone at 9.6 µm in altitude range 15–70 km, J. Geophys. Res., 114, D04306, doi:10.1029/2008JD010073, 2009. 12267, 12270

ACPD
13, 12263–12286, 2013
Solar cycle and stratospheric ozone
S. S. Dhomse et al.

Soukharev, B. E. and Hood, L. L.: Solar cycle variation of stratospheric ozone: Multiple regression analysis of long-term satellite data sets and comparisons with models, J. Geophys. Res., 111, D20314, doi:10.1029/2006JD007107, 2006. 12265, 12274
Terao, Y. and Logan, J. A.: Consistency of time series and trends of stratospheric ozone as seen by ozonesondes, SAGE II, HALOE, and SBUV(/2), J. Geophys. Res., 112, D06310, doi:10.1029/2006JD007667, 2007. 12275
Unruh, Y., Solanki, S., and Fligge, M.: The spectral dependence of facular contrast and solar irradiance variations, Astron. Astrophys., 345, 635–642, 1999. 12267
Wang, H. J., Froidevaux, L., Anderson, J., Schwartz, M., Fuller, R., Bernath, P., Zawodny, J. M., Thomason, L. W., Pawson, S., and Rienecker, M.: Long term stratospheric ozone record obtained by merging O_3 profiles from different satellites, SPARC/WMO Ozone Trend Workshop, Geneva, Switzerland, http://igaco-o3.fmi.fi/VDO/presentations_2011/datasets/WS_2011_Wang.pdf, last access: 25 November, 2011. 12275
Weber, M., Dhomse, S., Wittrock, F., Richter, A., Sinnhuber, B., and Burrows, J.: Dynamical control of NH and SH winter/spring total ozone from GOME observations in 1995–2002, Geophys. Res. Lett., 30, 1583, doi:10.1029/2002GL016799, 2003. 12274
WMO: Scientific Assessment of Ozone Depletion: 1985, Global Ozone Research and Monitoring Project Report 16, World Meteorological Organization, Geneva, 1985. 12268
Woods, T. N.: Solar irradiance variability: comparisons of observations over solar cycles 21–24, in: EGU General Assembly Conference Abstracts, edited by: Abbasi, A. and Giesen, N., Vol. 14, p. 1520, European Geosciences Union, Munich, Germany, 2012. 12269

ACPD
13, 12263–12286, 2013

ACPD
13, 12263–12286, 2013

Solar cycle and stratospheric ozone

S. S. Dhomse et al.

Table 1. Solar and dynamical conditions for the model simulations.

Run	Solar fluxes	Dynamics
A_NRL	NRL-SSI	ERA-interim
B_SATIRE	SATIRE-S	ERA-interim
C_FIX	Fixed (mean NRL-SSI, 2001–2010)	ERA-interim
D_SORCE2004	SORCE (2004)	ERA-interim
E_SORCE2007	SORCE (2007)	ERA-interim
G_NRLF	NRL-SSI	Fixed (year 2004)
F_SATIREF	SATIRE-S	Fixed (year 2004)

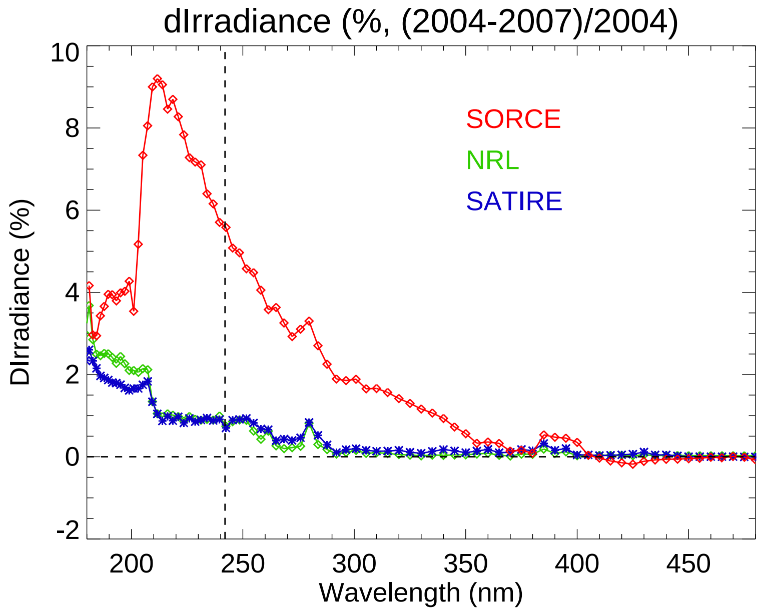

Fig. 1. Relative percentage differences in solar irradiance between 2004 and 2007 ((2004–2007)/2004) for the SORCE, NRL-SSI and SATIRE solar flux datasets. The threshold wavelength (242 nm) controlling O_3 production and destruction is also indicated with vertical dash line.

ACPD
13, 12263–12286, 2013

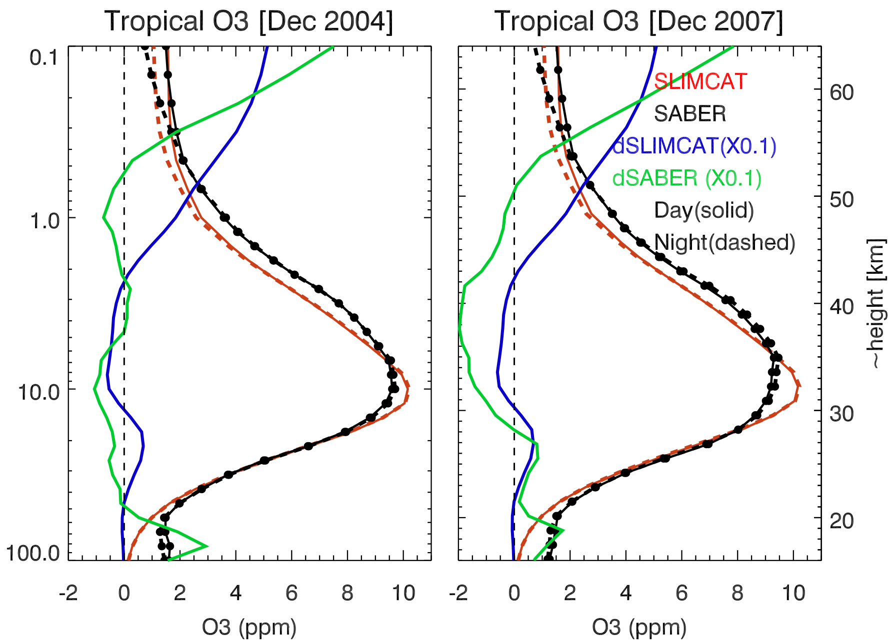

Fig. 2. Monthly mean tropical (25° S–25° N) O_3 profiles for December 2004 and December 2007 from SABER data (black) and SLIMCAT run *A_NRL* (orange). Solid and dashed lines represent day-time and night-time profiles, respectively. Also shown is the O_3 diurnal variation (day-night) for SABER (green) and SLIMCAT (blue). For clarity, the diurnal variations have been scaled by a factor of 10.

ACPD
13, 12263–12286, 2013

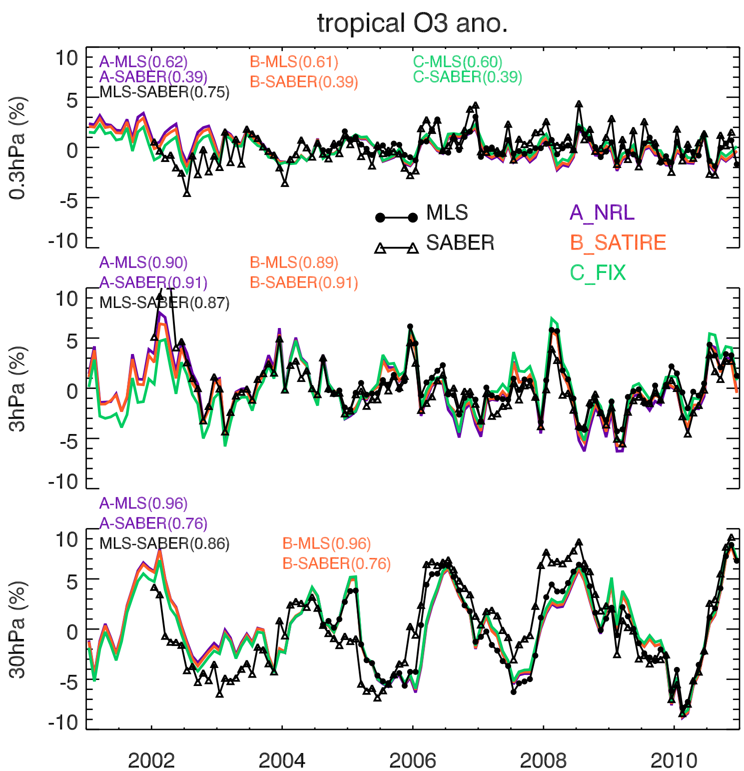

Fig. 3. Tropical (25° S–25° N) O_3 anomalies (%) from 3 model simulations (run *A_NRL* – violet, run *B_SATIRE* – orange, run *C_FIX* – green) and satellite data (MLS (2004–2010) – filled circles, SABER (2002–2010) – triangles) at 30 hPa (bottom), 3 hPa (middle) and 0.3 hPa (top). The rank-correlation between different O_3 anomalies is also given.

ACPD
13, 12263–12286, 2013

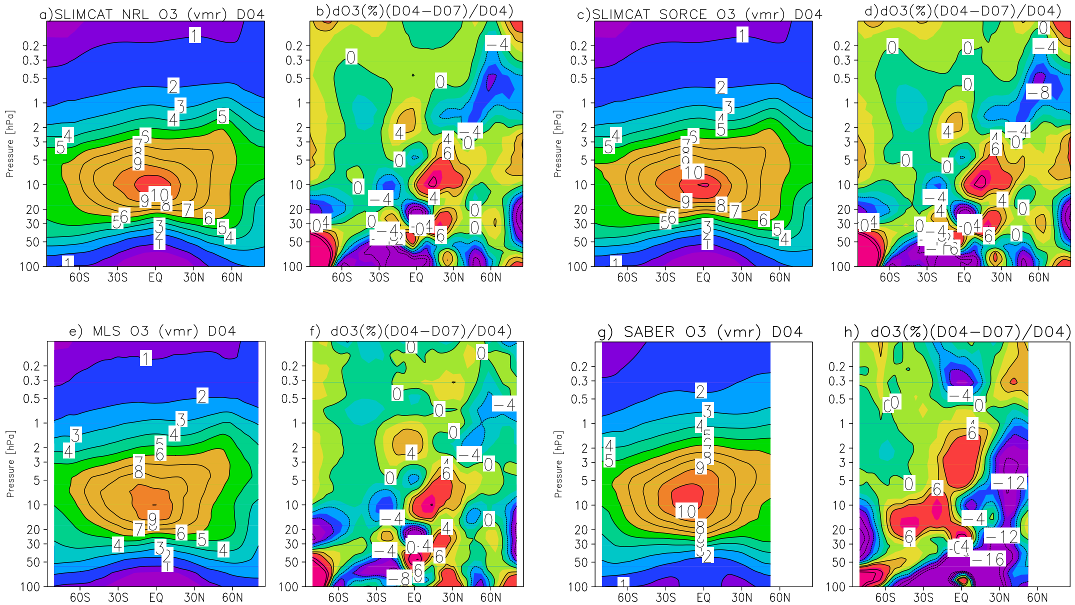

Fig. 4. Zonal mean monthly mean O_3 mixing ratio (ppmv) from SLIMCAT runs *A_NRL*, *D_SORCE2004* (panels **a** and **c**) and MLS and SABER (panels **e** and **g**) for December 2004. The ozone differences (%) between December 2004 and December 2007 for the corresponding data sets are also shown (panels **b**, **d**, **f**, **h**).

ACPD
13, 12263–12286, 2013

Solar cycle and stratospheric ozone

S. S. Dhomse et al.

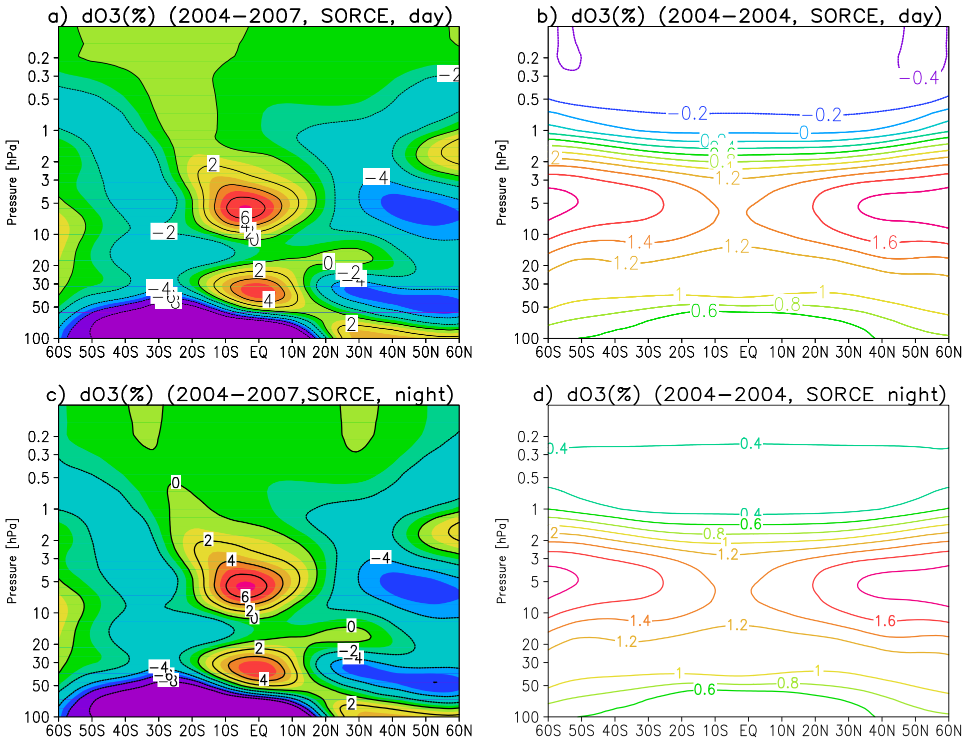

Fig. 5. (a) Differences in annual mean zonal mean O_3 between 2004 and 2007 for *D_SORCE2004* and *E_SORCE2007* in day-time (i.e. O_3 change due to both solar flux and dynamical variability). **(b)** Similar to **(a)** but for fixed meteorological forcing (year 2004, i.e. O_3 changes only due to solar flux variability). **(c)** and **(d)** are similar to **(a)** and **(b)**, respectively but for night-time O_3.

ACPD
13, 12263–12286, 2013

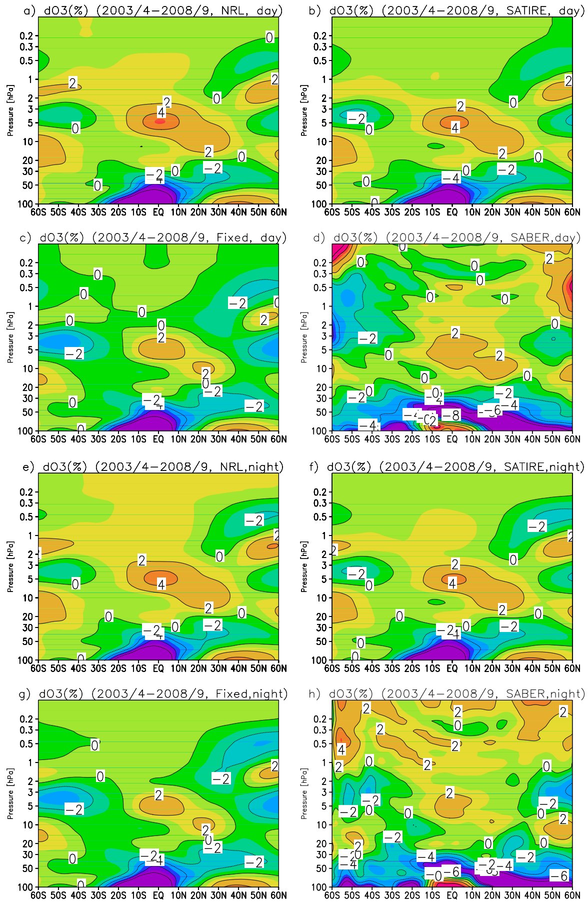

Fig. 6. Day-time (panels **a–d**) and night-time (panels **e–f**) biannual mean zonal mean O_3 differences (%) between 2003/2004 and 2008/2009 for (**a** and **e**) SLIMCAT run *A_NRL*, (**b** and **f**) SLIMCAT run *B_SATIRE*, (**c** and **g**) SLIMCAT run *C_FIX* and (**d** and **h**) SABER data.

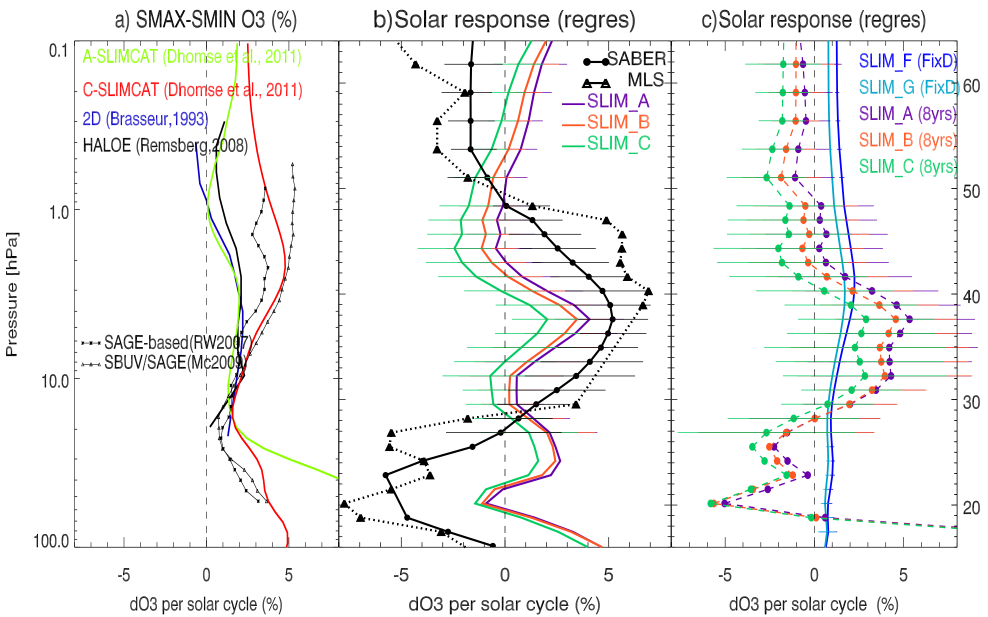

Fig. 7. (a) Tropical solar signal (25° S–25° N) per solar cycle from SLIMCAT simulations for 1979–2010 with ERA-40 and fixed dynamics (Dhomse et al., 2011, green and red lines), HALOE (1992–2005, Remsberg, 2008, black line) and a 2-D model (Brasseur, 1993, blue line). The estimated solar signal using SBUV/SAGE data (McLinden et al., 2009, triangles), SAGE-based data (Randel and Wu (2007), stars) and a 3-D model (light-green line) by Dhomse et al. (2011) for 1979–2005 are also shown. **(b)** Estimated solar signal using multivariate regression model for modelled (2001–2010, 120 months), SABER (2002–2010, 108 months) and MLS (2004–2010, 77 months) O_3 data sets. Estimated errors (1σ) for solar coefficients are shown with coloured horizontal lines. The large error bars (±10 %) at all levels for MLS data and in the lower stratosphere for SABER and model data are not shown. **(c)** The coloured dashed lines with filled circles show the solar signal from runs *A_NRL* and *B_SATIRE* if only 8 yr (2003–2010) of model data are used. The estimated solar signal from the runs (fixed dynamics) *G_NRLF* and *F_SATIREF* are shown with dark and light blue lines, respectively.

ACPD
13, 12263–12286, 2013